

scattering factors were taken from ref 36 with corrections applied for anomalous scattering. All calculations were carried out on a MicroVAX 3600 computer using the Glasgow GX suite of programs.<sup>37</sup>

**Acknowledgment.** Johnson Matthey is thanked for a

generous loan of platinum metal salts and the SERC for use of the solid-state NMR facility at Durham, U.K.

**Supplementary Material Available:** Figures 9 and 10, showing variable-temperature <sup>13</sup>C and <sup>31</sup>P NMR spectra of cluster 3e, and tables of anisotropic thermal parameters, calculated hydrogen positional parameters, and complete bond lengths, bond angles, and torsion angles (13 pages); a listing of calculated and observed structure factors (17 pages). Ordering information is given on any current masthead page.

(36) *International Tables for X-Ray Crystallography*; Kynoch: Birmingham, England, 1974; Vol. 4.

(37) Mallinson, P. R.; Muir, K. W. *J. Appl. Chem.* 1985, 18, 51.

## Synthesis, Structure, and Properties of a Tetranuclear Platinum Cluster Cation

Graeme Douglas,<sup>1a</sup> Ljubica Manojlovic-Muir,<sup>\*,1a</sup> Kenneth W. Muir,<sup>1a</sup> Michael C. Jennings,<sup>1b</sup> Brian R. Lloyd,<sup>1b</sup> Mehdi Rashidi,<sup>1b,c</sup> Guy Schoettel,<sup>1b</sup> and Richard J. Puddephatt<sup>\*,1b</sup>

Chemistry Department, University of Glasgow, Glasgow G12 8QQ, Scotland, and Department of Chemistry, University of Western Ontario, London, Ontario N6A 5B7, Canada

Received May 10, 1991

The reaction of [Pt(O<sub>2</sub>CCF<sub>3</sub>)<sub>2</sub>(dppm)] (dppm = Ph<sub>2</sub>PCH<sub>2</sub>PPh<sub>2</sub>) with CO/H<sub>2</sub>O at 100 °C gives the 58-electron cluster cation [Pt<sub>4</sub>(μ-H)(μ-CO)<sub>2</sub>(μ-dppm)<sub>3</sub>(dppm-P)]<sup>+</sup> (1). The structure of 1[PF<sub>6</sub>]<sup>-</sup> has been determined crystallographically (space group *Pcab* (No. 61), *a* = 21.120 (6) Å, *b* = 28.962 (4) Å, *c* = 31.026 (4) Å, *Z* = 8) and shown to contain a Pt<sub>4</sub> core in a butterfly geometry. The cluster cation can be considered to be derived from a triangular Pt<sub>3</sub>(μ-dppm)<sub>3</sub> unit, with one edge bridged above by a Pt(CO)<sub>2</sub>(dppm-P) unit and below by a proton. Variable-temperature <sup>1</sup>H, <sup>13</sup>C, <sup>31</sup>P, and <sup>195</sup>Pt NMR spectra show that the cluster cation 1 is fluxional, and the detailed mechanism of this fluxionality has been elucidated by analysis of the coupling constants to <sup>195</sup>Pt in the slow- and fast-exchange regions. The cluster core of 1 is robust, but it can be decomposed by H<sup>+</sup> or Ag<sup>+</sup> to give the cluster cation [Pt<sub>3</sub>(μ<sub>3</sub>-CO)(μ-dppm)<sub>3</sub>]<sup>2+</sup>. Methyl isocyanide displaces the carbonyl ligands of 1 to give [Pt<sub>4</sub>(μ-H)(μ-CNMe)<sub>2</sub>(μ-dppm)<sub>3</sub>(dppm-P)]<sup>+</sup> (4). The dppm-P ligand of 1 is easily oxidized by O<sub>2</sub> or H<sub>2</sub>O<sub>2</sub> to give [Pt<sub>4</sub>(μ-H)(μ-CO)<sub>2</sub>(μ-dppm)<sub>3</sub>(Ph<sub>2</sub>PCH<sub>2</sub>P(=O)Ph<sub>2</sub>)]<sup>+</sup> (5) and by S<sub>8</sub> or H<sub>2</sub>S to give [Pt<sub>4</sub>(μ-H)(μ-CO)<sub>2</sub>(μ-dppm)<sub>3</sub>(Ph<sub>2</sub>PCH<sub>2</sub>P(=S)Ph<sub>2</sub>)]<sup>+</sup> (6). The reagents Ph<sub>3</sub>PAu<sup>+</sup> and [Pt(O<sub>2</sub>CCF<sub>3</sub>)<sub>2</sub>(dppm)] react with 1 to give [Pt<sub>4</sub>(μ-AuPPh<sub>3</sub>)(μ-CO)<sub>2</sub>(μ-dppm)<sub>3</sub>(dppm-AuPPh<sub>3</sub>)]<sup>+</sup>[PF<sub>6</sub>]<sub>2</sub><sup>-</sup> (7[PF<sub>6</sub>]<sub>2</sub>) and [Pt<sub>4</sub>(μ-H)(μ-CO)<sub>2</sub>(μ-dppm)<sub>3</sub>(dppm-Pt(O<sub>2</sub>CCF<sub>3</sub>)(dppm))]<sup>+</sup>[PF<sub>6</sub>]<sub>2</sub><sup>-</sup> (8[PF<sub>6</sub>]<sub>2</sub>), respectively, by coordination to the dppm-P ligand and, in the case of the gold reagent, by isolobal substitution of LAu<sup>+</sup> for H<sup>+</sup>. These complexes have been characterized by multinuclear NMR methods.

### Introduction

Studies of the chemistry of platinum cluster complexes have been concentrated on the triplatinum clusters, which contain a triangle of platinum atoms.<sup>2-5</sup> However, many higher clusters are known and have been structurally characterized, and there are excellent reviews of this field.<sup>2-4,6</sup> Cluster bonding theories, adapted for platinum's tendency to have a 16-electron rather than 18-electron count, predict that a tetrahedral Pt<sub>4</sub> cluster will be favored for a 56-electron count and that higher electron counts will cause cleavage of metal-metal bonds and opening up of the cluster skeleton.<sup>2,7</sup> Most Pt<sub>4</sub> clusters have a 58-electron count, and in agreement with theory, they adopt a "butterfly" structure, which may be considered to be derived by opening one edge of a tetrahedron.<sup>2-4,7</sup> The clusters [Pt<sub>4</sub>(μ-CO)<sub>5</sub>(PR<sub>3</sub>)<sub>4</sub>] are good examples of such 58-electron butterfly clusters, and systematic studies have

been made of their synthesis, structural and spectroscopic properties, and chemical reactivity.<sup>2-4,8-11</sup>

This paper reports the synthesis of the new 58-electron Pt<sub>4</sub> cluster cation [Pt<sub>4</sub>(μ-H)(μ-CO)<sub>2</sub>(μ-dppm)<sub>3</sub>(dppm-P)]<sup>+</sup> (1; dppm = Ph<sub>2</sub>PCH<sub>2</sub>PPh<sub>2</sub>) together with a study of its structure, fluxionality, and chemical reactivity. A preliminary account of parts of this work has been published,<sup>12</sup> and the related neutral cluster [Pt<sub>4</sub>(μ-CO)<sub>2</sub>(μ-dppm)<sub>3</sub>(Ph<sub>2</sub>PCH<sub>2</sub>PPh<sub>2</sub>=O)] has also been reported.<sup>13</sup>

### Results and Discussion

**Synthesis of the Pt<sub>4</sub> Cluster.** The reduction of [Pt(O<sub>2</sub>CCF<sub>3</sub>)<sub>2</sub>(dppm)] by carbon monoxide (10 atm) in aqueous methanol at 100 °C gives a useful synthesis of the cluster cation [Pt<sub>3</sub>(μ<sub>3</sub>-CO)(μ-dppm)<sub>3</sub>]<sup>2+</sup> (2), whose chemistry is very rich.<sup>5</sup> At intermediate stages of reduction, diplatinum(I) complexes such as [Pt<sub>2</sub>H(CO)(μ-dppm)<sub>2</sub>]<sup>+</sup>

(1) (a) University of Glasgow. (b) University of Western Ontario. (c) Permanent address: Department of Chemistry, Shiraz University, Shiraz, Iran.

(2) Mingos, D. M. P.; Wardle, R. W. M. *Transition Met. Chem.* 1985, 10, 441.

(3) Eremko, N. K.; Mednikov, E. G.; Kurasov, S. S. *Russ. Chem. Rev. (Engl. Transl.)* 1985, 54, 394.

(4) Clark, H. C.; Jain, V. K. *Coord. Chem. Rev.* 1984, 55, 151.

(5) Puddephatt, R. J.; Manojlovic-Muir, Lj.; Muir, K. W. *Polyhedron* 1990, 9, 2767.

(6) Chini, P. *J. Organomet. Chem.* 1980, 200, 37.

(7) Sappa, E.; Tiripicchio, A.; Carty, A. J.; Toogood, G. E. *Prog. Inorg. Chem.* 1987, 35, 437.

(8) Vranka, R. G.; Dahl, L. F.; Chini, P.; Chatt, J. *J. Am. Chem. Soc.* 1969, 91, 1574.

(9) Chatt, J.; Chini, P. *J. Chem. Soc. A* 1970, 1538.

(10) Evans, D. G.; Hallam, M. F.; Mingos, D. M. P.; Wardle, R. W. M. *J. Chem. Soc., Dalton Trans.* 1987, 1889.

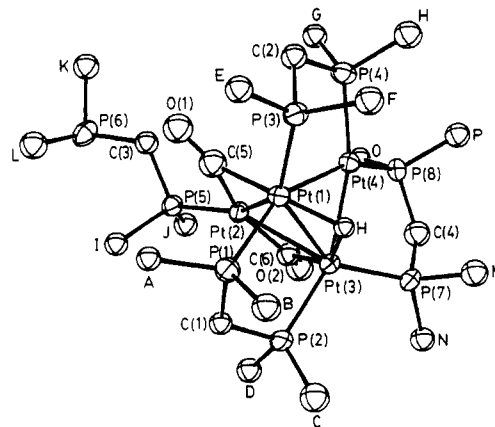
(11) Moor, A.; Pregosin, P. S.; Venanzi, L. M.; Welch, A. J. *Inorg. Chim. Acta* 1984, 85, 103.

(12) Douglas, G.; Manojlovic-Muir, Lj.; Muir, K. W.; Jennings, M. C.; Lloyd, B. R.; Rashidi, M.; Puddephatt, R. J. *J. Chem. Soc., Chem. Commun.* 1988, 149.

(13) Frew, A. A.; Hill, R. H.; Manojlovic-Muir, Lj.; Muir, K. W.; Puddephatt, R. J. *J. Chem. Soc., Chem. Commun.* 1982, 198.

**Table I. Selected Bond Lengths (Å) and Angles (deg) in 1[PF<sub>6</sub>]**

Bond Lengths			
Pt(1)-Pt(2)	2.750 (1)	Pt(1)-Pt(3)	2.705 (1)
Pt(1)-Pt(4)	2.620 (1)	Pt(1)-P(1)	2.360 (4)
Pt(1)-P(3)	2.266 (5)	Pt(1)-C(5)	2.089 (17)
Pt(1)-H(1)	1.69 (12)	Pt(2)-Pt(3)	2.720 (1)
Pt(2)-P(5)	2.250 (5)	Pt(2)-C(5)	1.971 (18)
Pt(2)-C(6)	1.980 (17)	Pt(3)-Pt(4)	2.613 (1)
Pt(3)-P(2)	2.329 (5)	Pt(3)-P(7)	2.254 (5)
Pt(3)-C(6)	2.146 (16)	Pt(3)-H(1)	2.02 (13)
Pt(4)-P(4)	2.257 (5)	Pt(4)-P(8)	2.256 (5)
P(1)-C(1)	1.766 (16)	P(2)-C(1)	1.839 (16)
P(3)-C(2)	1.826 (15)	P(4)-C(2)	1.853 (16)
P(5)-C(3)	1.825 (15)	P(6)-C(3)	1.848 (17)
P(7)-C(4)	1.837 (16)	P(8)-C(4)	1.834 (17)
O(1)-C(5)	1.212 (21)	O(2)-C(6)	1.170 (20)
P-C(phenyl) 1.803 (13)-1.855 (10)			
Bond Angles			
Pt(2)-Pt(1)-Pt(3)	59.8 (1)	Pt(2)-Pt(1)-Pt(4)	70.0 (1)
Pt(2)-Pt(1)-P(1)	99.5 (2)	Pt(2)-Pt(1)-P(3)	132.5 (2)
Pt(2)-Pt(1)-C(5)	45.6 (5)	Pt(2)-Pt(1)-H(1)	107.3 (41)
Pt(3)-Pt(1)-Pt(4)	58.7 (1)	Pt(3)-Pt(1)-P(1)	93.6 (2)
Pt(3)-Pt(1)-H(1)	48.3 (42)	Pt(4)-Pt(1)-P(1)	152.3 (2)
Pt(4)-Pt(1)-P(3)	89.5 (2)	Pt(4)-Pt(1)-C(5)	90.4 (5)
Pt(4)-Pt(1)-H(1)	66.3 (38)	P(1)-Pt(1)-P(3)	114.8 (2)
P(1)-Pt(1)-C(5)	100.2 (5)	P(1)-Pt(1)-H(1)	94.3 (38)
P(3)-Pt(1)-C(5)	94.6 (5)	P(3)-Pt(1)-H(1)	102.0 (42)
C(5)-Pt(1)-H(1)	150.9 (40)	Pt(1)-Pt(2)-Pt(3)	59.3 (1)
Pt(1)-Pt(2)-P(5)	146.9 (2)	Pt(1)-Pt(2)-C(5)	49.2 (5)
Pt(1)-Pt(2)-C(6)	110.3 (5)	Pt(3)-Pt(2)-P(5)	150.7 (2)
Pt(3)-Pt(2)-C(5)	108.4 (5)	Pt(3)-Pt(2)-C(6)	51.4 (5)
P(5)-Pt(2)-C(5)	99.5 (6)	P(5)-Pt(2)-C(6)	102.0 (5)
C(5)-Pt(2)-C(6)	157.8 (7)	Pt(1)-Pt(3)-Pt(2)	60.9 (1)
Pt(1)-Pt(3)-Pt(4)	59.0 (1)	Pt(1)-Pt(3)-P(2)	96.1 (2)
Pt(1)-Pt(3)-P(7)	141.0 (2)	Pt(1)-Pt(3)-C(6)	106.8 (5)
Pt(1)-Pt(3)-H(1)	38.6 (34)	Pt(2)-Pt(3)-Pt(4)	70.6 (1)
Pt(2)-Pt(3)-P(2)	93.4 (2)	Pt(2)-Pt(3)-P(7)	136.5 (2)
Pt(2)-Pt(3)-C(6)	46.2 (5)	Pt(2)-Pt(3)-H(1)	98.9 (34)
Pt(4)-Pt(3)-P(2)	154.5 (2)	Pt(4)-Pt(3)-P(7)	91.3 (2)
Pt(4)-Pt(3)-C(6)	88.8 (4)	Pt(4)-Pt(3)-H(1)	63.2 (31)
P(2)-Pt(3)-P(7)	113.4 (2)	P(2)-Pt(3)-C(6)	94.1 (5)
P(2)-Pt(3)-H(1)	101.6 (32)	P(7)-Pt(3)-C(6)	96.2 (5)
P(7)-Pt(3)-H(1)	107.8 (35)	C(6)-Pt(3)-H(1)	142.8 (33)
Pt(1)-Pt(4)-Pt(3)	62.3 (1)	Pt(1)-Pt(4)-P(4)	96.6 (2)
Pt(1)-Pt(4)-P(8)	155.7 (2)	Pt(3)-Pt(4)-P(4)	158.8 (2)
Pt(3)-Pt(4)-P(8)	94.0 (2)	P(4)-Pt(4)-P(8)	107.0 (2)
Pt(1)-P(1)-C(1)	108.1 (5)	Pt(3)-P(2)-C(1)	108.5 (5)
Pt(1)-P(3)-C(2)	108.7 (6)	Pt(4)-P(4)-C(2)	110.9 (5)
Pt(2)-P(5)-C(3)	113.0 (6)	Pt(3)-P(7)-C(4)	107.6 (6)
Pt(4)-P(8)-C(4)	112.0 (6)	P(1)-C(1)-P(2)	120.0 (9)
P(3)-C(2)-P(4)	109.2 (8)	P(5)-C(3)-P(6)	120.1 (9)
P(7)-C(4)-P(8)	114.5 (9)	Pt(1)-C(5)-Pt(2)	85.2 (7)
Pt(1)-C(5)-O(1)	133.1 (14)	Pt(2)-C(5)-O(1)	141.6 (14)
Pt(2)-C(6)-Pt(3)	82.4 (6)	Pt(2)-C(6)-O(2)	147.1 (13)
Pt(3)-C(6)-O(2)	130.1 (13)	Pt(1)-H(1)-Pt(3)	93.2 (56)

**Figure 1.** View of the structure of the cluster cation 1.**Table II. Selected NMR Data for the Cluster Cations at 20 °C**

	1	4	5	6	7 <sup>a</sup>	8 <sup>b</sup>
$\delta(\text{P}^{\text{a}}-\text{P}^{\text{c}})$	-21.5	-22.0	-21.4	-21.5	-22.1	-21.5
$^1J(\text{PtP})$ , Hz	3234	3255	3238	3214	2900	3210
$\delta(\text{P}^{\text{d}})$	18.8	17.4	15.3	17.4	15.0	21.5
$^1J(\text{PtP}^{\text{d}})$ , Hz	5400	5160	5580	5565	5200	5521
$^2J(\text{PtP}^{\text{d}})$ , Hz	336	342	345	345	330	316
$^3J(\text{P}^{\text{d}}\text{P}^{\text{e}})$ , Hz	15	15	14	17	50	40
$^2J(\text{P}^{\text{d}}\text{P}^{\text{e}})$ , Hz	73	55	13		20	
$\delta(\text{P}^{\text{e}})$	-31.6	-31.1	18.1	28.7	26.4	12.8
$^3J(\text{Pt}^{\text{e}}\text{P}^{\text{e}})$ , Hz	97	129	94	69	220	239
$\delta(\text{PtH})$	-7.4	-7.1	-7.6	-7.4		-7.5
$J(\text{PtH})$ , Hz	508	507	501	510		512
$^2J(\text{Pt}^{\text{h}}\text{H})$ , Hz	24	30	25	20		24

<sup>a</sup>  $\delta(\text{AuPPh}_3) = 39.0$  [ $^2J(\text{P}^{\text{e}}\text{P}^{\text{f}}) = 325$  Hz,  $\text{P}^{\text{f}}$ ], 39.6 [ $\mu\text{-AuPPh}_3$ ].  
<sup>b</sup>  $^1J(\text{Pt}^{\text{d}}\text{P}^{\text{e}}) = 1840$  Hz.  $\delta(\text{P}^{\text{h}}) = -47.01$  [ $^1J(\text{PtP}) = 2120$  Hz,  $^2J(\text{P}^{\text{e}}\text{P}^{\text{h}}) = 402$  Hz,  $^2J(\text{P}^{\text{d}}\text{P}^{\text{e}}) = 63$ ] Hz;  $\delta(\text{P}^{\text{e}}) = -58.4$  [ $^1J(\text{PtP}) = 3200$  Hz,  $^2J(\text{P}^{\text{e}}\text{P}^{\text{e}}) = 10$  Hz].

appears that hydrogen formed in the WGS reaction is necessary for the formation of 1. The hydride cluster  $[\text{Pt}_3(\mu_3\text{-H})(\mu\text{-dppm})_3]^+$  (3) is believed to be involved in the catalytic cycle of the WGS reaction, and it is likely that the last step in the formation of 1 is the reaction of 3 with "Pt(CO)<sub>2</sub>(dppm)". Complex 1 could be crystallized as the hexafluorophosphate salt, and in the solid state, it was stable to air; in solution, slow oxidation of the  $\eta^1$ -dppm ligand occurred but the cluster core was retained. The cation 1 is a 58-electron Pt<sub>4</sub> cluster.

**Structure of the Pt<sub>4</sub> Cluster 1[PF<sub>6</sub>].** Red crystals of 1[PF<sub>6</sub>], whose structure was determined by X-ray diffraction, were grown from acetone/pentane and they are made up of well-separated cations and anions. The structure of the cation is shown in Figure 1 and is characterized by bond distances and angles shown in Table I.

The cluster cation 1 contains a butterfly arrangement of four platinum atoms. Thus, of the six Pt-Pt vectors, five, with lengths in the range 2.613 (1)-2.750 (1) Å, correspond to metal-metal bonds.<sup>2-5</sup> However, the Pt(2)-Pt(4) distance of 3.082 (1) Å is outside the usual range for Pt-Pt bonds.<sup>2-4</sup> The hinge torsion angle Pt(2)-Pt(1)-Pt(3)-Pt(4) of 83.7 (1)° lies between the values of 70.5° in a regular tetrahedron and those of 89.4 and 96.8° found in different crystalline forms of  $[\text{Pt}_4(\text{CO})_5(\text{PMe}_2\text{Ph})_4]$ .<sup>8,11</sup>

The atoms Pt(1)Pt(3)Pt(4) in 1 define a triangle whose edges are bridged by three  $\mu$ -dppm ligands so that the resulting Pt<sub>3</sub>P<sub>6</sub> unit is roughly planar. On opposite sides of this plane, the Pt(1)-Pt(3) bond is further bridged by a Pt(CO)<sub>2</sub>(dppm-P) fragment and by a  $\mu$ -H ligand. The  $\mu$ -H ligand was located in a difference electron density map, and its parameters were refined successfully. Both

can be detected, and these are probably formed by reaction of the short-lived platinum(0) intermediate  $[\text{Pt}(\text{dppm})(\text{CO})_n]$  with a platinum(II) complex. The trinuclear complex 2 is then formed by reaction of more platinum(0) complex  $[\text{Pt}(\text{dppm})(\text{CO})_n]$  with  $[\text{Pt}_2\text{H}(\text{CO})(\mu\text{-dppm})_2]^+$ . All these platinum complexes act as catalysts or catalyst precursors for the water-gas shift (WGS) reaction, and so hydrogen is continuously formed in the reaction pressure vessel. Unless this hydrogen was occasionally purged by fresh carbon monoxide during the above reaction, it was discovered that a further reduction of 2 occurred to give the Pt<sub>4</sub> cluster cation  $[\text{Pt}_4(\mu\text{-H})(\mu\text{-CO})_2(\mu\text{-dppm})_3(\text{dppm-P})]^+$  (1) often in very high yield. The simplest equation describing the formation of 1 is given in eq 1 (X = CF<sub>3</sub>CO<sub>2</sub>). However, this is an oversimplification, since it

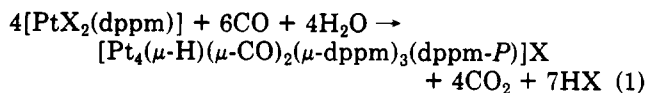
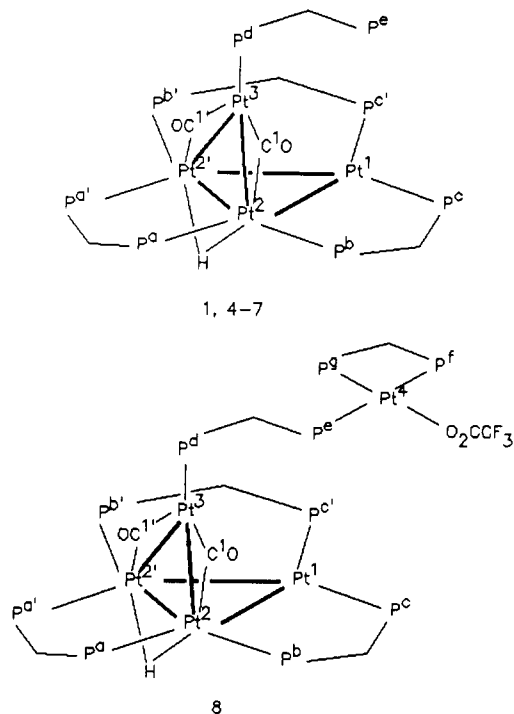


Chart I. NMR Labeling Scheme for 1 (with Minor Changes, 4-7) and 8



carbonyl ligands are present in an unsymmetrical  $\mu_2$ -CO bonding mode. Thus, the Pt(2)-C(5) and Pt(2)-C(6) bond distances of 1.97 (2) and 1.98 (2) Å are shorter than the Pt(1)-C(5) and Pt(3)-C(6) distances of 2.09 (2) and 2.15 (2) Å, respectively, indicating that the carbonyls are more strongly bound to Pt(2). The carbonyl carbon atoms are displaced by 0.1–0.2 Å from the Pt(1)Pt(2)Pt(3) plane toward Pt(4). Each of the  $Pt_2(\mu\text{-dppm})$  groups adopts an envelope conformation with the  $CH_2$  flap directed above the Pt(1)Pt(3)Pt(4) plane toward the Pt(2)(CO)<sub>2</sub>(dppm-P) unit. Hence, all the phenyl groups on this side of the plane are equatorial, while those on the hydride side are axial. This clearly minimizes steric hindrance between phenyl groups and the bulkier Pt(2)(CO)<sub>2</sub>(dppm-P) unit.<sup>5</sup>

Of the Pt-Pt bonds, the shortest are those with no single-atom bridging group (Pt(1)-Pt(4) = 2.620 (1), Pt(3)-Pt(4) = 2.613 (1) Å) and the longest are the carbonyl-bridged bonds (Pt(1)-Pt(2) = 2.750 (1), Pt(2)-Pt(3) = 2.720 (1) Å); the hydride-bridged bond has an intermediate length of 2.705 (1) Å.

**Spectra and Fluxionality of the Cluster Cation 1.** The NMR spectra of 1 are particularly complex and informative and so will be discussed in detail. The NMR labeling scheme is shown in the line drawing of 1 (Chart I) and is different from the X-ray labeling (Figure 1).

The symmetry of the cation 1 was most readily determined from the <sup>31</sup>P NMR spectra (Figure 2). At room temperature, three resonances in a 1:1:6 intensity ratio were observed due to P<sup>d</sup>, P<sup>e</sup>, and P<sup>a</sup>-P<sup>c</sup>, respectively. This shows that the dppm-P ligand is rigidly bonded to Pt<sup>2</sup> but that there is a fluxional process which makes all <sup>31</sup>P atoms of the Pt<sub>3</sub>(μ-dppm)<sub>3</sub> unit effectively equivalent. The cluster thus appears to have C<sub>3v</sub> symmetry on the NMR time scale. At -40 °C, the broad resonance in the <sup>31</sup>P NMR spectrum due to the μ-dppm phosphorus atoms split into three resonances, as expected for the nonequivalent phosphorus atoms P<sup>a</sup>, P<sup>b</sup>, and P<sup>c</sup> of the static structure 1. The appearance of the P<sup>d</sup> resonance also changed at low temperature (Figure 2, insets). At room temperature, the inner resonance appears as a 1:4:7:4:1 quintet of 1:1

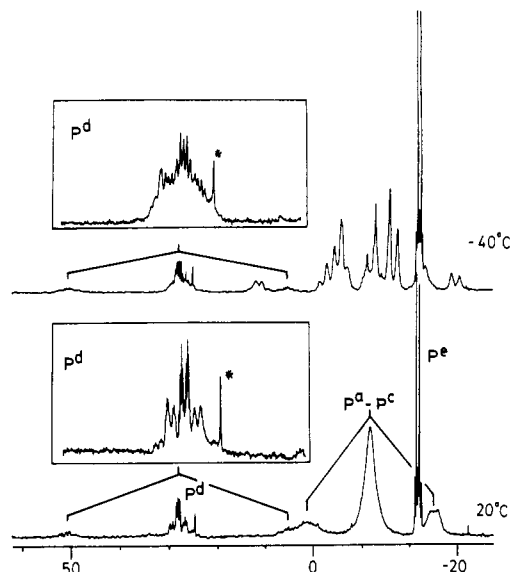


Figure 2. <sup>31</sup>P NMR spectra (121.5 MHz) of 1: (above) -40 °C; (below) 20 °C. Expansions of the P<sup>d</sup> resonance are shown in the insets.

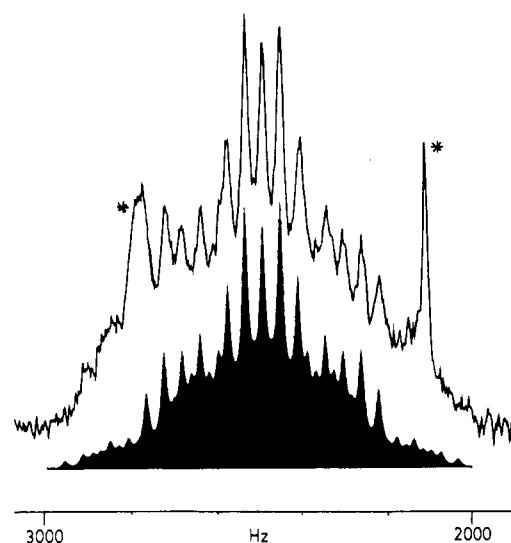
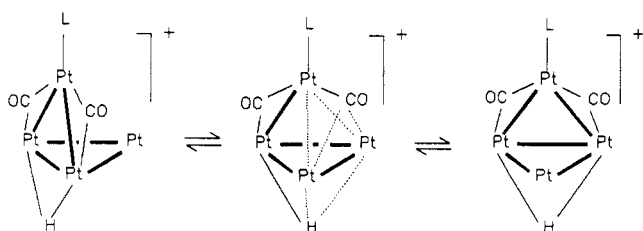


Figure 3. (Above) Expansion of the P<sup>d</sup> NMR resonance of 1 at -40 °C. (Below) Computer simulation, with use of the parameters given in the text.

doublets, and there are also outer satellites of one-fourth intensity due to  $^1J(\text{Pt}^3\text{P}^d)$ . The doublet is due to  $^2J(\text{P}^d\text{P}^e)$ , while the apparent 1:4:7:4:1 quintet is due to equal coupling of P<sup>d</sup> to the three platinum atoms Pt<sup>1</sup>, Pt<sup>2</sup>, and Pt<sup>2'</sup> with the observed coupling  $J(\text{Pt}^d\text{P}) = 336$  Hz. Theoretically, coupling to three equivalent platinum atoms should give a 1:12:49:84:49:12:1 septet, but the outer lines are too weak to observe, and so an apparent 1:4:7:4:1 quintet is observed.<sup>14</sup> At low temperature, the long-range PtP coupling gives rise to a 1:8:18:8:1 quintet of 1:4:1 triplets due to the couplings  $^2J(\text{Pt}^2\text{P}^d) = ^2J(\text{Pt}^2'\text{P}^d)$  and  $^3J(\text{Pt}^1\text{P}^d)$ , respectively. This is not immediately apparent because the appearance of the resonance (Figure 2) is so complex, but the assignments were confirmed by simulation as shown in Figure 3. The couplings  $^2J(\text{Pt}^2\text{P}^d) = ^2J(\text{Pt}^2'\text{P}^d)$  and  $^3J(\text{Pt}^1\text{P}^d)$  were 378 and 252 Hz, respectively, and the "average" coupling is therefore expected to be  $\frac{1}{3}(2 \times 378 + 252) = 336$  Hz, in excellent agreement with the observed

(14) Bradford, A. M.; Douglas, G.; Manojlovic-Muir, Lj.; Muir, K. W.; Puddephatt, R. J. *Organometallics* 1990, 9, 409.

Scheme I



value of 336 Hz (see above).

The  $^1\text{H}$  NMR spectrum in the PtH region showed a similar temperature dependence (Figure 4). Thus, at room temperature the PtH resonance appeared as an apparent 1:4:7:4:1 quintet due to PtH coupling with observed  $J(\text{PtH}) = 508$  Hz, but at  $-40^\circ\text{C}$  it appeared as a 1:8:18:8:1 quintet of 1:4:1 triplets due to  $^1J(\text{Pt}^2\text{H}) = ^1J(\text{Pt}^2\text{H}) = 670$  Hz and  $^2J(\text{Pt}^1\text{H}) = 168$  Hz, respectively. The observed  $J(\text{PtH})$  value in the region of rapid fluxionality should therefore be  $1/3(2 \times 670 + 168) = 503$  Hz, in good agreement with the experimental value.

The complex  $1[\text{PF}_6]$  underwent slow exchange of  $^{12}\text{CO}$  by  $^{13}\text{CO}$  when a solution was allowed to stand under a  $^{13}\text{CO}$  atmosphere for 2 days. The  $^{13}\text{C}$  NMR spectrum of the  $^{13}\text{CO}$ -labeled complex  $1^*$  was also temperature dependent (Figure 5). At  $-40^\circ\text{C}$ , the resonance appeared as a 1:4:1 triplet of 1:4:1 triplets due to  $^1J(\text{Pt}^3\text{C}) = 820$  Hz and  $^1J(\text{Pt}^3\text{C}^1) = 390$  Hz, respectively, and the magnitudes of these couplings are as expected from the respective Pt-C distances ( $\text{Pt}^3\text{C} = 1.97\text{--}1.98$ ,  $\text{Pt}^2\text{C} = 2.09\text{--}2.15$  Å). At room temperature, the 1:4:1 triplet due to  $^1J(\text{Pt}^3\text{C})$  was unchanged but an apparent 1:4:7:4:1 quintet with observed  $J(\text{PtC}) = 130$  Hz was also present (the satellites being much broader than the central resonance; Figure 5). This is due to equal couplings to  $\text{Pt}^1$ ,  $\text{Pt}^2$ , and  $\text{Pt}^2'$  as a result of the fluxionality.

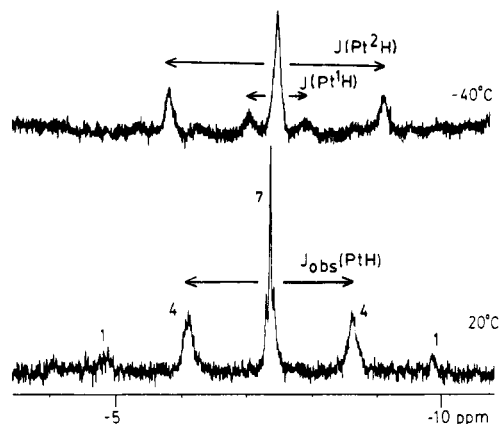
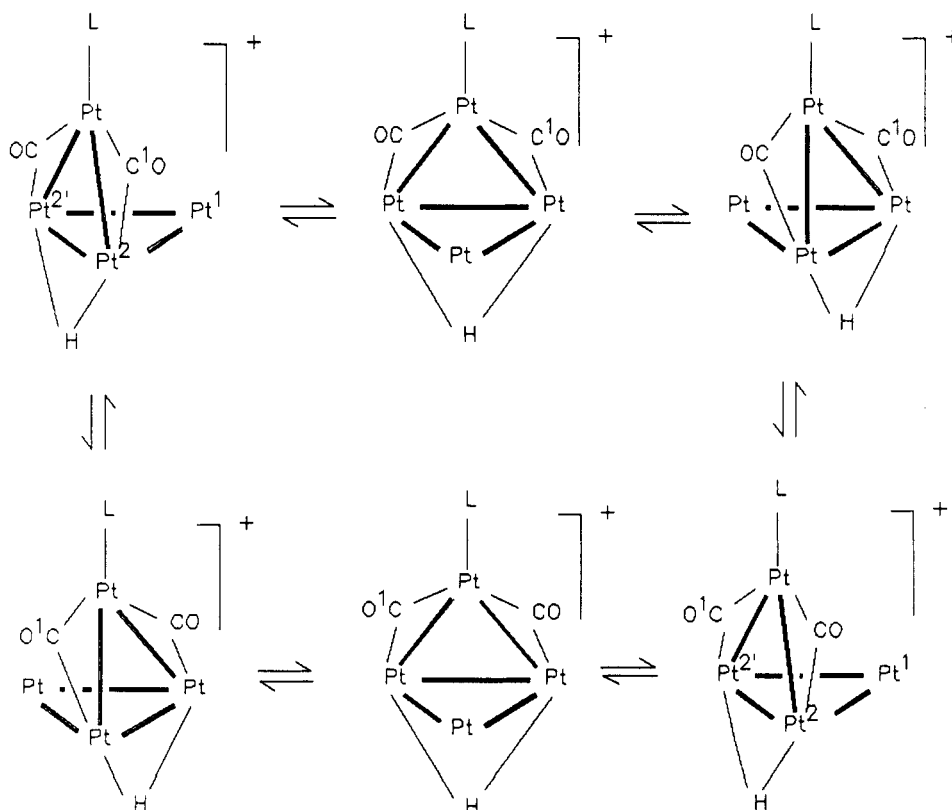


Figure 4.  $^1\text{H}$  NMR spectra of **1** in the hydride region: (above)  $-40^\circ\text{C}$ ; (below)  $20^\circ\text{C}$ .

An attempt was made to study the fluxionality by using  $^{195}\text{Pt}$  NMR spectroscopy, but this was not successful. At room temperature and at  $-40$  and  $-80^\circ\text{C}$ , the  $\text{Pt}^3$  resonance appeared as a broad doublet with  $^1J(\text{Pt}^3\text{P}^d) = 5400$  Hz, but the resonances due to  $\text{Pt}^1$  and  $\text{Pt}^2$  were not observed. It is probable that the fluxionality causes the line broadening of these peaks to be so great that they cannot be resolved.

The above NMR data, especially the temperature dependence of the observed coupling constants to  $^{195}\text{Pt}$ , define clearly the mechanism of fluxionality. The  $\text{Pt}_3$  triangle of the  $\text{Pt}_3(\mu\text{-dppm})_3$  unit is of course rigidly bound by the  $\mu\text{-dppm}$  ligands, but the  $\mu\text{-H}$  and  $\text{Pt}^3(\text{CO})_2(\text{dppm-P})$  groups can evidently migrate from edge to edge of the  $\text{Pt}_3$  triangle as shown in Scheme I ( $\mu\text{-dppm}$  groups omitted for clarity), which shows one such edge-to-edge migration via a tetrahedral  $\text{Pt}_4$  cluster intermediate. There are six equivalent structures **1**, corresponding to six  $60^\circ$  rotations

Scheme II



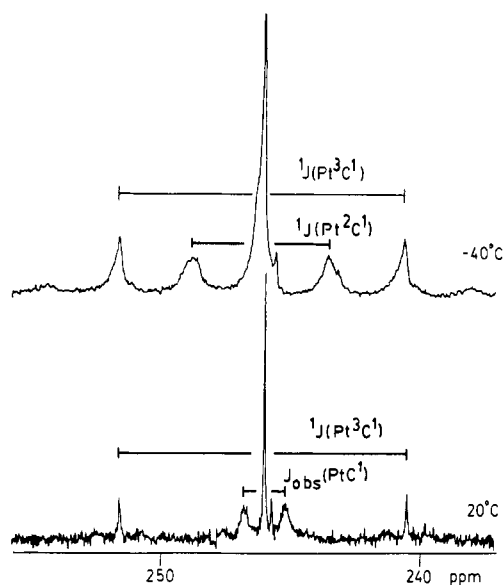
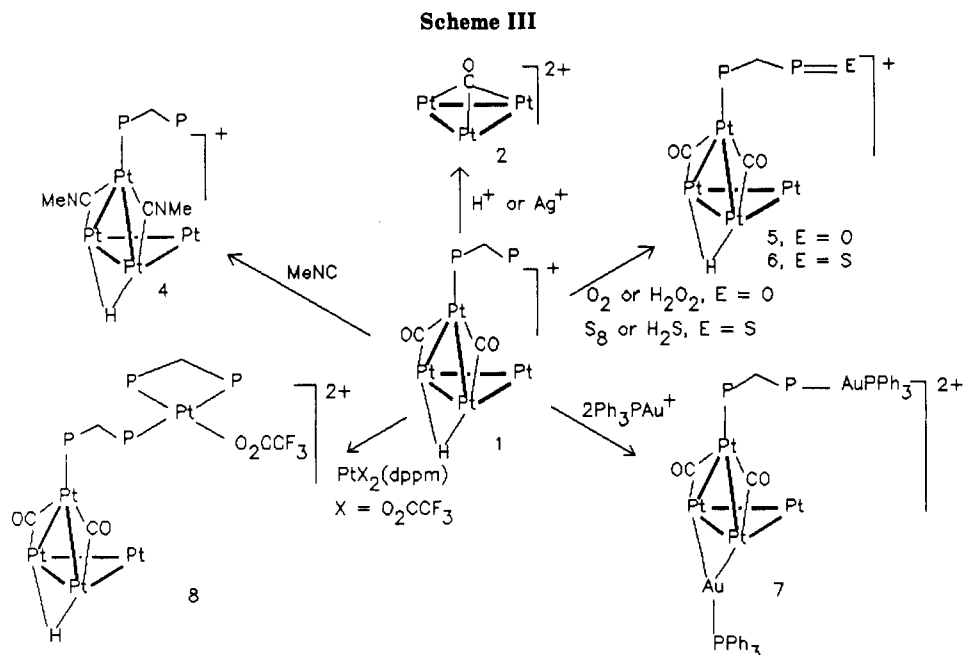


**Figure 5.**  $^{13}\text{C}$  NMR spectra (75.4 MHz) of **1** in the carbonyl region: (above)  $-40^\circ\text{C}$ ; (below)  $20^\circ\text{C}$ .

as illustrated in Scheme II. Since the  $\text{Pt}^{\text{d}}$  and  $\text{Pt}^{\text{c}}$  bonds remain intact throughout the rotations, the corresponding coupling constants are not temperature dependent, but the couplings of  $\text{P}^{\text{d}}$  and  $\text{C}^1$  to  $\text{Pt}^1$ ,  $\text{Pt}^2$ , and  $\text{Pt}^3$  change in the expected way. The temperature dependence of the  $\text{PtH}$  couplings to the hydride resonance is also rationalized by the mechanism of Scheme I.

Finally, the  $^1\text{H}$  resonances due to the  $\text{CH}_2\text{P}_2$  protons of the  $\mu$ -dppm ligands are also informative. At room temperature these occur as an "AB" quartet. Thus, as expected, all  $\mu$ -dppm ligands are effectively equivalent but the  $\text{CH}^{\text{a}}\text{H}^{\text{b}}$  protons of each remain distinct. This is because the fluxional process does not create an effective plane of symmetry containing the  $\text{Pt}_3(\mu\text{-dppm})_3$  unit. At low temperature, each of the  $\text{CH}_2$  peaks splits into two in a 2:1 ratio as expected for the structure **1**. From the coalescence temperature, the activation energy for the fluxional process is estimated as  $50 \pm 1 \text{ kJ mol}^{-1}$ . The fluxionality of the complexes  $[\text{Pt}_4(\mu\text{-CO})_5\text{L}_4]$  ( $\text{L} = \text{PR}_3$ ) occurs with a lower activation energy, such that it is rapid even at  $-80^\circ\text{C}$  and gives effective equivalence of all  $^{195}\text{Pt}$ ,  $^{31}\text{P}$ , and  $^{13}\text{C}$  atoms

in the NMR spectra.<sup>11</sup> Such a general exchange cannot occur in **1** because of the presence of the  $\mu$ -dppm ligands, which lock the  $\text{Pt}_3(\mu\text{-dppm})_3$  unit in place. For both **1** and  $[\text{Pt}_4(\mu\text{-CO})_5\text{L}_4]$  a tetrahedral  $\text{Pt}_4$  skeleton is thought to be present in the transition state, but otherwise, the proposed mechanisms are significantly different.<sup>11</sup>

The  $\text{Pt}_3(\mu\text{-dppm})_3$  unit models some of the properties of a triangle of platinum atoms on a  $\text{Pt}(111)$  surface,<sup>5</sup> and the easy migrations of the hydride ligand and  $\text{Pt}^3$  atom around the  $\text{Pt}_3$  triangle of **1** may model similar surface migration processes, which may be involved in catalytic hydrogenation by platinum or surface reconstruction of platinum, respectively.

**Chemistry of the Cluster Cation 1.** The cluster core of **1** is remarkably robust. For example, the cluster core of **1** was not affected by reaction with  $\text{H}_2\text{S}$ , which easily causes cleavage of  $\text{Pt}\text{-Pt}$  bonds in binuclear and trinuclear platinum complexes.<sup>5,15,16</sup> In addition, **1** failed to react with mild bases such as  $\text{Et}_3\text{N}$  to give the deprotonated cluster  $[\text{Pt}_4(\mu\text{-CO})_2(\mu\text{-dppm})_3(\text{dppm}\text{-P})]^+$ ,<sup>13</sup> though stronger bases such as  $\text{MeLi}$  caused decomposition. Several reactions did occur and are shown in Scheme III.

As described above, the carbonyl ligands of **1** can be exchanged by  $^{13}\text{C}$  and the similar displacement of  $\text{CO}$  ligands by  $\text{MeNC}$  gives  $[\text{Pt}_4(\mu\text{-H})(\mu\text{-CNMe})_2(\mu\text{-dppm})_3(\text{dppm}\text{-P})]^+$  (**4**). In the  $^1\text{H}$  NMR spectrum, the  $\text{MeNC}$  protons of **4** give a singlet with  $^{195}\text{Pt}$  satellites and otherwise the NMR spectra were similar to those of **1**.

The monodentate dppm ligand of **1** was oxidized by  $\text{O}_2$  or  $\text{H}_2\text{O}_2$  to give  $[\text{Pt}_4(\mu\text{-H})(\mu\text{-CO})_2(\mu\text{-dppm})_3(\text{Ph}_2\text{PCH}_2\text{P}(=\text{O})\text{Ph}_2)]^+$  (**5**) or by  $\text{H}_2\text{S}$  or  $\text{S}_8$  to give  $[\text{Pt}_4(\mu\text{-H})(\mu\text{-CO})_2(\mu\text{-dppm})_3(\text{Ph}_2\text{PCH}_2\text{P}(=\text{S})\text{Ph}_2)]^+$  (**6**). The chief effect on the NMR spectra was a change in  $^{31}\text{P}$  chemical shift of the dangling phosphorus in **1** ( $-31.6 \text{ ppm}$ ) to  $18.1 \text{ ppm}$  in **5** (Figure 6) and  $28.7 \text{ ppm}$  in **6**. Complexes **4**–**6** all display fluxionality as described in detail for **1**.

The cluster **1** reacted cleanly with  $\text{CF}_3\text{CO}_2\text{H}$  or with  $\text{AgPF}_6$  to give  $[\text{Pt}_3(\mu_3\text{-CO})(\mu\text{-dppm})_3]^{2+}$  (**2**) with loss of the fourth platinum atom. This reaction is useful since at-

(15) Jennings, M. C.; Payne, N. C.; Puddephatt, R. J. *Inorg. Chem.* 1987, 26, 3776.

(16) Hadji-Bagheri, N.; Puddephatt, R. J.; Manojlovic-Muir, Lj.; Stefanovic, A. *J. Chem. Soc., Dalton Trans.* 1990, 535.

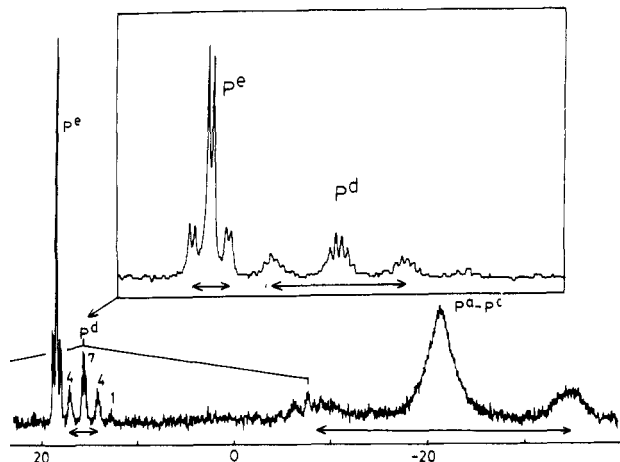


Figure 6. The  $^{31}\text{P}$  NMR spectrum of complex 5.

tempted syntheses of **2** often give **1** as an impurity, and **1** can be removed by reaction of the impure mixture with  $\text{CF}_3\text{CO}_2\text{H}$ . Alternatively, formation of **1** can be prevented by carrying out the reduction of  $[\text{Pt}(\text{O}_2\text{CCF}_3)_2(\text{dppm})]$  by  $\text{CO}/\text{H}_2\text{O}$  to give **2** in the presence of  $\text{CF}_3\text{CO}_2\text{H}$ .

The reaction of **1** [ $\text{PF}_6$ ] with 2 equiv of  $\text{Ph}_3\text{PAu}^+$  occurred cleanly to give  $[\text{Pt}_4(\mu\text{-AuPPh}_3)(\mu\text{-CO})_2(\mu\text{-dppm})_3(\text{dppm-AuPPh}_3)]_2[\text{PF}_6]_2$  (**7** [ $\text{PF}_6$ ] $_2$ ). This reaction involves displacement of the  $\mu\text{-H}$  ligand by the isolobal  $\text{Ph}_3\text{PAu}$  ligand and coordination of the dangling dppm ligand to gold. The dangling dppm ligand of **1** [ $\text{PF}_6$ ] could also be used to displace a trifluoroacetate ligand from  $[\text{Pt}(\text{O}_2\text{CCF}_3)_2(\text{dppm})]$  to give, after treatment with  $\text{NH}_4\text{PF}_6$ ,  $[\text{Pt}_4(\mu\text{-H})(\mu\text{-CO})_2(\mu\text{-dppm})_3(\text{dppm-Pt}(\text{O}_2\text{CCF}_3)(\text{dppm}))]_2[\text{PF}_6]_2$  (**8** [ $\text{PF}_6$ ] $_2$ ). Although these are complex molecules, the analytical and the rich NMR data define the structures clearly.

### Experimental Section

$^1\text{H}$  NMR spectra were recorded by using a Varian XL200 spectrometer and  $^{13}\text{C}$ ,  $^{31}\text{P}$ , and  $^{195}\text{Pt}$  NMR spectra by using a Varian XL300 spectrometer. References used were TMS ( $^1\text{H}$  and  $^{13}\text{C}$ ),  $\text{H}_3\text{PO}_4$  ( $^{31}\text{P}$ ), and aqueous  $\text{K}_2[\text{PtCl}_4]$  ( $^{195}\text{Pt}$ ).

**[Pt<sub>4</sub>(μ-H)(μ-CO)<sub>2</sub>(μ-dppm)<sub>3</sub>(dppm-P)]** [ $\text{PF}_6$ ] (**1** [ $\text{PF}_6$ ]). A mixture of  $[\text{Pt}(\text{O}_2\text{CCF}_3)_2(\text{dppm})]$  (1.0 g), MeOH (50 mL), and distilled  $\text{H}_2\text{O}$  (4 mL) in a Parr pressure reactor (300 mL) was heated at 100 °C for 3 days under CO (4 atm). The resulting red solution was evaporated under vacuum, the residue was dissolved in MeOH (5 mL), and this solution was added to a solution of  $\text{NH}_4[\text{PF}_6]$  (1.3 g) in MeOH (4 mL) to give the product as an orange-red precipitate, which was recrystallized from acetone/MeOH; yield 80%. Anal. Calcd for  $\text{C}_{102}\text{H}_{89}\text{F}_6\text{O}_2\text{P}_9\text{Pt}_4$ : C, 48.6; H, 3.6. Found: C, 48.5; H, 3.8. IR (Nujol mull):  $\nu(\text{CO}) = 1808, 1767 \text{ cm}^{-1}$ ; for **1**<sup>\*</sup>,  $\nu(^{13}\text{CO}) = 1764, 1728 \text{ cm}^{-1}$ . FAB MS: calcd for  $\text{Pt}_4\text{H}(\text{CO})_2(\text{dppm})_4^+$ ,  $m/e$  2375; found,  $m/e$  2375. NMR ( $J$  values in Hz):  $^1\text{H}$ ,  $\delta = 3.5$  [2 H,  $^2J(\text{PH}) = 10$ ,  $^3J(\text{PtH}) = 45$ ,  $\text{CH}_2$  of monodentate dppm], 3.96 [3 H,  $^2J(\text{PH}) = 11$ ,  $^3J(\text{PtH}) = 48$ ,  $\text{CH}^a\text{H}^b$  of  $\mu\text{-dppm}$ ], 5.80 [3 H,  $^2J(\text{PtH}) = 70$ ,  $\text{CH}^a\text{H}^b$  of  $\mu\text{-dppm}$ ];  $^{13}\text{C}$ ,  $\delta = 246$  [CO];  $^{31}\text{P}$  at  $-40$  °C,  $\delta = -21.8$  [2 P,  $^1J(\text{PtP}) = 2484$ ,  $^2J(\text{Pt}^1\text{P}^a) = 105$ ,  $^3J(\text{P}^a\text{P}^c) = 199$ ,  $\text{P}^a$ ],  $-15.2$  [2 P,  $^1J(\text{PtP}^b) = 4102$ ,  $^2J(\text{Pt}^3\text{P}^b) = 160$ ,  $^3J(\text{P}^b\text{P}^b) = 144$ ,  $\text{P}^b$ ],  $-26.0$  [2 P,  $^1J(\text{PtP}^c) = 3136$ ,  $^3J(\text{P}^a\text{P}^c) = 199$ ,  $\text{P}^c$ ], 18.2 [1 P,  $^1J(\text{PtP}) = 5400$ ,  $^2J(\text{PtP}^d) = 378$ ,  $^3J(\text{Pt}^1\text{P}^d) = 252$ ,  $^3J(\text{P}^d\text{P}^b) = 41$ ,  $\text{P}^d$ ],  $-31.6$  [ $^3J(\text{PtP}^e) = 80$ ,  $\text{P}^e$ ].

**[Pt<sub>4</sub>(μ-H)(μ-CNMe)<sub>2</sub>(μ-dppm)<sub>3</sub>(dppm-P)]** [ $\text{PF}_6$ ] (**4** [ $\text{PF}_6$ ]). A solution of MeNC in acetone (60  $\mu\text{L}$ , 0.29 M) was added to a solution of **1** [ $\text{PF}_6$ ] (50 mg) in acetone (10 mL), and the mixture was stirred at room temperature for 22 h at room temperature. The solvent was evaporated under vacuum to give the product as a red solid, which was crystallized from acetone/pentane. Anal. Calcd for  $\text{C}_{104}\text{H}_{95}\text{F}_6\text{N}_2\text{P}_9\text{Pt}_4$ : C, 49.1; H, 3.8. Found: C, 48.4; H, 3.7. NMR:  $^1\text{H}$ ,  $\delta = 3.53$  [6 H,  $^4J(\text{PtH}) = 22.5$ , MeN], 4.07 [2 H, monodentate dppm], 3.37 [3 H,  $^2J(\text{PH}) = 10$ ,  $\text{CH}^a\text{H}^b$  of  $\mu\text{-dppm}$ ], 6.55 [3 H,  $^2J(\text{PH}) = 10$ ,  $^3J(\text{PtH}) = 72$ ,  $\text{CH}^a\text{H}^b$ ].

Table III. Crystallographic Data for  $[\text{Pt}_4(\mu\text{-H})(\mu\text{-CO})_2(\mu\text{-dppm})_3(\text{dppm-P})]_2[\text{PF}_6]_2$

formula	$\text{C}_{102}\text{H}_{89}\text{F}_6\text{O}_2\text{P}_9\text{Pt}_4$
$M_r$	2519.9
space group	$Pcab$ (No. 61)
$a/\text{Å}$	21.120 (6)
$b/\text{Å}$	28.962 (4)
$c/\text{Å}$	31.026 (4)
$V/\text{Å}^3$	18978 (6)
$Z$	8
$d(\text{calc})/\text{g cm}^{-3}$	1.764
cryst dimens/(mm)	$0.48 \times 0.48 \times 0.08$
temp/°C	23
radiation (wavelength/Å)	Mo K $\alpha$ (0.71069)
$\mu(\text{Mo K}\alpha)/\text{cm}^{-1}$	61.5
$F(000)$	9744
data collec range ( $2\theta$ )/deg	0–23
no. of unique rflns with $I \geq 3\sigma(I)$	6261
no. of params refined	385
$R$	0.038
$R_w$	0.045

**[Pt<sub>4</sub>(μ-H)(μ-CO)<sub>2</sub>(μ-dppm)<sub>3</sub>(Ph<sub>2</sub>PCH<sub>2</sub>P(=O)Ph<sub>2</sub>)]** [ $\text{PF}_6$ ] (**5** [ $\text{PF}_6$ ]). To a solution of **1** [ $\text{PF}_6$ ] (50 mg) in acetone (2 mL) was added  $\text{H}_2\text{O}_2$  solution (3 drops, 50%). After 10 min at room temperature, diethyl ether (10 mL) was added to precipitate the product; yield 94%. Anal. Calcd for  $\text{C}_{102}\text{H}_{89}\text{F}_6\text{O}_3\text{P}_9\text{Pt}_4$ : C, 48.3; H, 3.5. Found: C, 47.9; H, 3.7. IR (Nujol mull):  $\nu(\text{CO}) = 1807, 1770 \text{ cm}^{-1}$ . FAB MS: calcd for  $\text{Pt}_4\text{H}(\text{CO})_2(\text{dppm})_3(\text{dppm}=\text{O})^+$ ,  $m/e$  2391; found,  $m/e$  2391. The same complex was prepared by reaction of **1** [ $\text{PF}_6$ ] in acetone with  $\text{O}_2$  (1 atm) for 1 week.

**[Pt<sub>4</sub>(μ-H)(μ-CO)<sub>2</sub>(μ-dppm)<sub>3</sub>(Ph<sub>2</sub>PCH<sub>2</sub>P(=S)Ph<sub>2</sub>)]** [ $\text{PF}_6$ ] (**6** [ $\text{PF}_6$ ]). **6** [ $\text{PF}_6$ ] was similarly prepared from **1** [ $\text{PF}_6$ ] and  $\text{H}_2\text{S}$ . Anal. Calcd for  $\text{C}_{102}\text{H}_{89}\text{F}_6\text{O}_2\text{P}_9\text{Pt}_4\text{S}$ : C, 48.0; H, 3.5. Found: C, 47.8; H, 3.5. IR (Nujol mull):  $\nu(\text{CO}) = 1804, 1757 \text{ cm}^{-1}$ . FAB MS: calcd for  $\text{Pt}_4\text{H}(\text{CO})_2(\text{dppm})_3(\text{dppm}=\text{S})^+$ ,  $m/e$  2407; found,  $m/e$  2407.

**[Pt<sub>4</sub>(μ-AuPPh<sub>3</sub>)(μ-CO)<sub>2</sub>(μ-dppm)<sub>3</sub>(dppm-AuPPh<sub>3</sub>)]** [ $\text{PF}_6$ ] $_2$  (**7** [ $\text{PF}_6$ ] $_2$ ). A solution of  $[\text{Au}(\text{NO}_3)(\text{PPh}_3)]$ , freshly prepared from  $[\text{AuCl}(\text{PPh}_3)]$  (40 mg) in  $\text{CH}_2\text{Cl}_2$  (5 mL) and  $\text{AgNO}_3$  (14.4 mg) in  $\text{H}_2\text{O}/\text{EtOH}$  (6 mL), was filtered and then added dropwise to a solution of **1** [ $\text{PF}_6$ ] (104 mg) in  $\text{CH}_2\text{Cl}_2$  (15 mL). After 5 min, the solution was washed with aqueous  $\text{NH}_4\text{PF}_6$ , dried over  $\text{MgSO}_4$ , and then evaporated and crystallized from  $\text{CH}_2\text{Cl}_2$ /ether. Anal. Calcd for  $\text{C}_{139}\text{H}_{118}\text{Au}_2\text{F}_{12}\text{P}_{12}\text{Pt}_4$ : C, 46.3; H, 3.3. Found: C, 46.7; H, 3.2. IR (Nujol):  $\nu(\text{CO}) = 1806, 1759 \text{ cm}^{-1}$ . NMR:  $^1\text{H}$ ,  $\delta = 3.89$  [2 H,  $\text{CH}_2$ ], 4.04 [3 H,  $\text{CH}^a\text{H}^b$ ], 6.46 [3 H,  $\text{CH}^a\text{H}^b$ ].

**[Pt<sub>4</sub>(μ-H)(μ-CO)<sub>2</sub>(μ-dppm)<sub>3</sub>(dppm-Pt(O<sub>2</sub>CCF<sub>3</sub>)(dppm))]** [ $\text{PF}_6$ ] $_2$  (**8** [ $\text{PF}_6$ ] $_2$ ). To a solution of **1** [ $\text{PF}_6$ ] (50 mg) in acetone (2 mL) was added  $[\text{Pt}(\text{O}_2\text{CCF}_3)(\text{dppm})]$  (17 mg) in acetone (3 mL). After 30 min,  $\text{NH}_4\text{PF}_6$  (10 mg) was added and  $\text{Et}_2\text{O}$  (10 mL) was added to precipitate the product. Anal. Calcd for  $\text{C}_{129}\text{H}_{111}\text{F}_{15}\text{O}_4\text{P}_{12}\text{Pt}_5$ : C, 46.15; H, 3.3. Found: C, 46.0; H, 3.3. IR (Nujol mull):  $\nu(\text{CO}) = 1807, 1768 \text{ cm}^{-1}$ . FAB MS: calcd for  $\text{Pt}_5\text{H}(\text{CO})_2(\text{dppm})_5^+$ ,  $m/e$  2952; found,  $m/e$  2952.

**X-ray Crystal Structure Analysis of [Pt<sub>4</sub>(μ-H)(μ-CO)<sub>2</sub>(μ-dppm)<sub>3</sub>(dppm-P)]** [ $\text{PF}_6$ ] (**1** [ $\text{PF}_6$ ]). Cherry red plates of **1** [ $\text{PF}_6$ ] were obtained from acetone solution by slow evaporation. All X-ray measurements were made with graphite-monochromated molybdenum radiation on an Enraf-Nonius CAD4 diffractometer.

The intensities of all reflections in the  $+h, +k, +l$  octant with  $\theta(\text{Mo K}\alpha) \leq 23^\circ$  were measured by  $\theta/2\theta$  scans of  $0.70^\circ$  in  $\theta$ , increased at each end by 25% to allow for background effects. A total of 6261 intensities, corrected empirically for absorption,<sup>17</sup> with  $I \geq 3\sigma(I)$ , were used in the analysis.

The structure was solved by direct and difference Fourier methods. At a late stage of refinement the bridging hydrogen atom H(1) was located as a prominent feature in a low-angle difference synthesis. Its positional and isotropic displacement parameters were refined by least squares. Full-matrix least-squares refinement of 385 parameters converged ( $\Delta/\sigma < 0.3$ ) at  $R = 0.038$  and  $R_w = 0.045$ . The following constraints were applied in the final refinement: (a) 16 phenyl rings were refined as rigid groups idealized as hexagons of side 1.38 Å; (b) the [ $\text{PF}_6$ ] anion

(17) Walker, N.; Stuart, D. *Acta Crystallogr., Sect. A: Found. Crystallogr.* 1983, A39, 158.

**Table IV. Fractional Atomic Coordinates and Isotropic Displacement Parameters ( $\text{\AA}^2$ ) for  $1[\text{PF}_6]$** 

	$x/a$	$y/b$	$z/c$	$U^a$
Pt(1)	0.30279 (3)	0.09876 (2)	0.33122 (2)	0.027
Pt(2)	0.24673 (3)	0.13707 (2)	0.40280 (2)	0.028
Pt(3)	0.17853 (3)	0.08408 (2)	0.34727 (2)	0.028
Pt(4)	0.21659 (3)	0.15875 (2)	0.30775 (2)	0.028
P(1)	0.3342 (2)	0.0271 (1)	0.3605 (1)	0.035
P(2)	0.1926 (2)	0.0172 (1)	0.3879 (2)	0.036
P(3)	0.3692 (2)	0.1278 (1)	0.2807 (1)	0.031
P(4)	0.2839 (2)	0.2106 (1)	0.2785 (1)	0.036
P(5)	0.2608 (2)	0.1687 (1)	0.4683 (1)	0.033
P(6)	0.3493 (2)	0.2396 (2)	0.5184 (2)	0.047
P(7)	0.0831 (2)	0.0882 (1)	0.3150 (1)	0.035
P(8)	0.1194 (2)	0.1910 (1)	0.3067 (1)	0.033
O(1)	0.3833 (5)	0.1625 (4)	0.3870 (4)	0.052 (3)
O(2)	0.1046 (6)	0.1354 (4)	0.4162 (4)	0.53 (3)
C(1)	0.2775 (7)	0.0105 (4)	0.3994 (5)	0.030 (4)
C(2)	0.3670 (7)	0.1908 (5)	0.2836 (5)	0.036 (4)
C(3)	0.3141 (7)	0.2182 (5)	0.4676 (5)	0.037 (4)
C(4)	0.0569 (8)	0.1486 (5)	0.3173 (5)	0.045 (5)
C(5)	0.3334 (8)	0.1432 (5)	0.3800 (6)	0.046 (5)
C(6)	0.1543 (8)	0.1258 (5)	0.4020 (5)	0.036 (4)
H(1)	0.245 (6)	0.076 (4)	0.301 (4)	0.02 (4)

<sup>a</sup> For Pt, P, and F atoms,  $U$  is the equivalent isotropic displacement parameter defined as  $U = 1/3 \sum_{i=1,3} \sum_{j=1,3} U_{ij} b_i b_j (\mathbf{a}_i \cdot \mathbf{a}_j)$ , where  $b_i$  is the  $i$ th reciprocal cell edge and  $\mathbf{a}_i$  is the  $i$ th direct cell vector.

was also refined as a rigid group in which the F atoms defined an octahedron centered on the P atom with P-F = 1.53  $\text{\AA}$ ; (c) phenyl and methylene hydrogen positions were deduced geometrically, a fixed contribution for the scattering of these atoms was added to the structure factors, and  $U(\text{H}) = 0.050 \text{\AA}^2$  was

assumed; (d) anisotropic displacement parameters were used only for Pt, P, and F atoms. All calculations were performed with use of the locally developed GX program package.<sup>18</sup>

Complex, neutral atom scattering factors were taken from ref 19. Function values in the final difference synthesis ranged from  $-0.83$  to  $+0.97 \text{ e \AA}^{-3}$ . Crystallographic data are given in Table III, fractional atomic coordinates and isotropic displacement parameters in Table IV, anisotropic displacement parameters in Table S1, calculated fractional coordinates and assumed isotropic displacement parameters ( $\text{\AA}^2$ ) for phenyl and methylene H atoms in Table S2, and the structure amplitudes in Table S3 (Tables S1-S3 are in the supplementary material).

**Acknowledgment.** We thank the SERC (U.K.) for a research studentship (to G.D.), NSERC (Canada) for financial support (to R.J.P.), and NATO for a travel grant.

**Registry No.**  $1[\text{PF}_6]$ , 118444-65-8;  $4[\text{PF}_6]$ , 136676-31-8;  $5[\text{PF}_6]$ , 136705-06-1;  $6[\text{PF}_6]$ , 136705-08-3;  $7[\text{PF}_6]$ , 136705-10-7;  $8[\text{PF}_6]$ , 136705-12-9; dppm, 2071-20-7;  $[\text{Pt}(\text{O}_2\text{CCF}_3)_2(\text{dppm})]$ , 99642-82-7;  $[\text{Au}(\text{NO}_3)(\text{PPh}_3)]$ , 14897-32-6;  $^{196}\text{Pt}$ , 14191-88-9.

**Supplementary Material Available:** Table S1 (anisotropic displacement parameters) and Table S2 (complete fractional coordinates for all atoms and calculated fractional coordinates and assumed isotropic displacement parameters ( $\text{\AA}^2$ ) for phenyl and methylene H atoms) (6 pages); Table S3 (structure amplitudes) (31 pages). Ordering information is given on any current masthead page.

(18) Mallinson, P. R.; Muir, K. W. *J. Appl. Crystallogr.* **1985**, *18*, 51.

(19) *International Tables for X-ray Crystallography*; Kynoch Press: Birmingham, England, 1974; Vol. IV.

## New Routes to $\text{Co}^{\text{I}}$ -Bis(diphenylphosphino)methane-Carbonyl Complexes Containing Monocoordinated and Chelating Ligands: Structure of $[\text{Co}(\eta^2\text{-dppm})_2(\text{CO})][\text{Co}(\text{CO})_4]$

David J. Elliot,<sup>1a,b</sup> David G. Holah,<sup>1a</sup> Alan N. Hughes,<sup>\*1a</sup> Vincent R. Magnuson,<sup>1c</sup>  
Irene M. Moser,<sup>1c</sup> Richard J. Puddephatt,<sup>1b</sup> and Wei Xu<sup>1a</sup>

Departments of Chemistry, Lakehead University, Thunder Bay, Ontario, Canada P7B 5E1,  
University of Western Ontario, London, Ontario, Canada N6A 5B7, and University of Minnesota—Duluth,  
Duluth, Minnesota 55812-2496

Received May 17, 1991

The mechanism of reduction of  $\text{Co}^{\text{II}}$  by  $\text{NaBH}_4$  in the presence of CO and dppm ( $\text{Ph}_2\text{PCH}_2\text{PPh}_2$ ), which can give any one or more of several  $\text{Co}^{\text{I}}$ ,  $\text{Co}^0$ , or  $\text{Co}^{\text{I-}}$  complexes depending upon experimental conditions, has been elucidated by detailed study of possible individual steps of the reaction. Reactions of  $\text{CoX}(\eta^1\text{-dppm})_3$  ( $\text{X} = \text{Cl}, \text{Br}$ ) with CO lead in sequence to  $\text{CoX}(\eta^1\text{-dppm})_2(\text{CO})_2$ ,  $[\text{Co}(\eta^2\text{-dppm})(\eta^1\text{-dppm})(\text{CO})_2]\text{X}$ , and  $[\text{Co}(\eta^2\text{-dppm})_2(\text{CO})]\text{X}$ , all of which have been isolated and fully characterized, and the series of reactions can be reversed under CO at elevated temperatures. The related complex  $[\text{Co}(\eta^1\text{-dppm})(\text{CO})_4]\text{Br}$  is formed by a modification of the procedure. The synthesis and X-ray crystal structure of  $[\text{Co}(\eta^2\text{-dppm})_2(\text{CO})][\text{Co}(\text{CO})_4]$  (1), formed in the direct reduction of the  $\text{CoX}_2/\text{dppm}/\text{CO}$  system by  $\text{NaBH}_4$ , are reported, and evidence for the reaction sequence whereby 1 is formed is presented. The heterobinuclear complex  $[\text{CoRh}(\mu\text{-dppm})_2(\mu\text{-CO})(\text{CO})_2(\mu\text{-Cl})]\text{Cl}$  has been synthesized by reaction of  $\text{CoCl}(\eta^1\text{-dppm})_2(\text{CO})_2$  with  $\text{Rh}_2(\text{CO})_4\text{Cl}_2$ . An X-ray diffraction investigation showed that 1 crystallizes in space group  $P2_1/a$  with  $a = 25.737 (6) \text{\AA}$ ,  $b = 11.129 (2) \text{\AA}$ ,  $c = 18.085 (3) \text{\AA}$ ,  $\alpha = 99.06 (2)^\circ$ , and  $Z = 4$ .

### Introduction

Reactions of  $\text{Co}^{\text{II}}$  salts with  $\text{NaBH}_4$  or  $\text{NaBH}_3\text{CN}$  in the presence of bis(diphenylphosphino)methane (dppm) have been shown<sup>2</sup> to give a variety of products depending upon

the reaction conditions. These products include the tetrahedral  $\text{Co}^{\text{I}}$  species  $\text{CoX}(\eta^1\text{-dppm})_3$  ( $\text{X} = \text{Cl}, \text{Br}$ ),  $\text{Co}^{\text{III}}$  complexes of the type  $[\text{CoHX}(\eta^2\text{-dppm})_2]^+$  ( $\text{X} = \text{Cl}, \text{Br}, \text{I}, \text{BH}_3\text{CN}$ ), and the mixed oxidation state system

(1) (a) Lakehead University. (b) University of Western Ontario. (c) University of Minnesota—Duluth.

(2) Elliot, D. J.; Holah, D. G.; Hughes, A. N.; Maciaszek, S.; Magnuson, V. R.; Parker, K. O. *Can. J. Chem.* **1988**, *66*, 81.